Chronic Neural Stimulation with Thin-Film, Iridium Oxide Electrodes

James D. Weiland*, *Member, IEEE,* and David J. Anderson, *Member, IEEE*

***Abstract*—Experiments were conducted to assess the effect of chronic stimulation on the electrical properties of the electrode-tissue system, as measured using electrochemical impedance spectroscopy (EIS) and cyclic voltammetry (CV). Silicon, micromachined probes with multiple iridium oxide stimulating electrodes (400–1600 μm^2) were implanted in guinea pig cortex. A 10–17 day post-operative recovery period was followed by five days of monopolar stimulation, two hours/electrode each day using biphasic, constant current stimulation (5–100 μA, 100 μs/phase). EIS and CV data were taken before and after stimulation. The post-stimulation impedance [at mid-range frequencies (100 Hz–100 kHz)] consistently and significantly decreased relative to prestimulation levels. Impedance magnitude increased permanently at low frequencies (<100 Hz), correlating to a change in the charge storage capacity (the area under a cyclic voltammagram). Impedance magnitude significantly increased during the recovery period, though this increase could be mostly reversed by applying small currents. A mathematical model of the electrode-tissue system impedance was used to analyze in vivo behavior. The data and modeling results shows that applying charge to the electrode can consistently reduce the impedance of the electrode-tissue system. Analysis of explanted probes suggests that the interaction between the tissue and electrode is dependent on whether chronic pulses were applied. It is hypothesized that the interface between the tissue and metal is altered by current pulsing, resulting in a temporary impedance shift.**

***Index Terms*—Electrical stimulation, impedance spectroscopy, iridium oxide, neural prosthesis, stimulating electrodes.**

I. Introduction

ELECTRICAL stimulation of nerve cells is complicated by the fact that electrical charge is carried by electrons in metal and by ions in aqueous neural tissue. Furthermore, single electrons cannot exist in solution, nor can ions flow through metal. This incompatibility is resolved at the metal–electrolyte interface, where charge is transferred or rearranged to allow current to effectively flow from metal to tissue. The efficacy of charge transfer will define the impedance of the interface and effect the design of the neural prosthesis. The electrode potential that results when a current pulse is applied to the electrode will largely determine power consumption and supply voltage, two considerations for the electronics of a neural prosthetic device. Understanding the *in vivo* behavior of stimulating electrodes is the first step in designing a more efficient interface, and thereby a more efficient prosthesis.

The charge carrying capacity of iridium electrodes can be increased by an order of magnitude by forming iridium oxide on the electrode surface [1]. Iridium oxide can be formed by cycling the electrode potential of iridium between positive and negative limits, a procedure that causes more oxide to grow with each cycle [1]. The result is a porous, hydrous, multilayer oxide film with characteristics that make it an attractive material for electrical stimulation of neural tissue ([2], [3]). Iridium oxide can dissipate charge through reversible Faradaic reactions that transfer charge ([4]–[8]). Reversibility means that no new substance is formed and hence no harmful reactants are released into tissue. For the purposes of this paper, safe stimulation current is defined as the amount of current that will result in no harmful reactant being produced at the electrode interface. That is, safe stimulation is defined in terms of the electrode. The actual mechanisms of neural injury are more complex and are related to both charge density and total charge per phase [9].

When a current pulse is applied to an electrode, the voltage developed across the interface is dependent upon the ability of the electrode to store or dissipate charge. The potential across the interface will increase as charge is applied to the electrode, which will result in more iridium oxide transferring to a higher valence by ejecting protons into the solution [3], [10]. The reaction below summarizes the sequential change in the oxide as potential increases (1). The IrO_3 state ($n = 3$) is unstable and its degradation will result in O_2 evolution. The reaction reverses as charge is subsequently removed from the oxide with a cathodic pulse. The nature of the reaction within the oxide film has two consequences. First, it makes iridium oxide superior to other metals in terms of maximum, safe stimulation current. The maximum charge deliverable with iridium oxide electrodes is 3 mC/cm^2 [4]. Platinum can safely inject 0.4 mC/cm^2 [8]. Secondly, it makes the characteristics of iridium oxide highly dependent on the electrode potential [11], [12]. Greater safe charge delivery limits can be attained by poising the electrode potential at a positive potential and applying a cathodic current pulse [4]. While measuring the properties of the electrode it is important to use a method that controls the voltage (i.e., a potentiostatic method), so that changes in electrode properties due to a change in electrode potential are not misinterpreted [11]

$$IrO_{n-1}(OH)_{4-n} \Leftrightarrow IrO_n(OH)_{3-n} + H^+ + e^-. \quad (1)$$

One way of analyzing the electrode properties would be to apply a current pulse and measure the resultant voltage drop between current source and current sink of the stimulator (the back

Manuscript received March 18, 1999; revised February 1, 2000. This work was supported by the National Institutes of Health (NIH) under Neural Prosthesis Program Grant NIH-NINDS-N01-NS-5-2335 and the Center for Neural Communication Technology under Grant NCRR/NIH P41 RR09754-04. *Asterisk indicates corresponding author.*

*J. D. Weiland is with the Wilmer Eye Institute, Johns Hopkins University, 600N Wolfe Street, Baltimore, MD 21287 USA (e-mail: jweiland@jhmi.edu).

D. J. Anderson with Electrical Engineering and Biomedical Engineering, University of Michigan, Ann Arbor, MI 48109 USA (e-mail: dja@engin.umich.edu).

Publisher Item Identifier S 0018-9294(00)05131-4.

voltage). Back voltage is the sum of several potentials that result from current flow along a complex path which includes the following elements: metal conducting lines from stimulator to electrode, the electrode-electrolyte interface, the neural tissue, and the return electrode. Back voltage will define the compliance voltage of the current generator electronics, and therefore is of great interest to the designers of neural prosthetic devices [13]. Analysis of the voltage response of platinum-iridium electrodes has been performed [14]. However, unless a near perfectly square current pulse is applied, these results can be difficult to interpret. Most commercial current pulse generators have a rise time of 10 μs. Additionally, the magnitude of the current pulse may provide sufficient energy to modify the properties of the interface at the same time these properties are being measured. Finally, the current pulse will change the electrode potential significantly, altering the electrode properties.

Iridium oxide and the surrounding neural tissue form an electrochemical interface [15]. Therefore, electrochemical measurement techniques can be used to assess the electrode-tissue system. Electrochemical impedance spectroscopy (EIS) and cyclic voltammetry (CV) are two potentiostatic methods used to evaluate electrochemical systems. EIS excites the interface with a small voltage sine wave ($<$20-mV rms) superimposed over a constant dc potential. The measured current through the test electrode determines the impedance of the system at the particular frequency. With modern instrumentation, a wide frequency range (1 mHz–1 MHz) is available to assess the properties of all parts of the electrode-tissue system. In addition to electrode characterization, EIS is widely used to evaluate dielectrics, corrosion reactions, and biological coatings ([11], [16], [17]). CV assesses electrode properties as a function of electrode potential by applying a slow triangle wave over a large potential range (e.g., 100 mV/s between -700 and 600 mV). The current measured during the voltage ramp reflects capacitive charging of the double layer and oxidation–reduction reactions that occur as the electrode potential changes.

Analysis of the impedance spectra allows the formation of circuit models of the interface. Since these circuit model parameters are also dependent on frequency and current density, applying circuit models over a wide range of frequencies is difficult [18]. Constant current impedance measurement would eliminate the error from current density, but introduce another source of error since iridium oxide conductivity is dependent on electrode potential. The nonlinearity due to current density is most significant at low frequencies ($<$1 kHz). Frequencies greater than 1 kHz are of interest for modeling current pulses, and for these frequencies, current density error is minimal [18]. For these reasons, a potentiostatic method was chosen over a galvanostatic (constant current) for electrode impedance evaluation.

A series of chronic animal experiments was undertaken to investigate the properties of the electrode-tissue system under conditions of electrical stimulation. A silicon probe with multiple iridium oxide stimulating sites was implanted in guinea pig cortex. Electrochemical measurements (EIS and CV) of the electrode sites were made before and after several hours of pulsed current, charge balanced stimulation. The EIS data were used to formulate and quantify circuit models of the interface.

II. Experimental Methods

A. Silicon Stimulating Probes

Silicon stimulating probes manufactured with integrated circuit technology were used in this study, the details of which are available elsewhere [19]. The device is a two-dimensional "pitchfork" array, with site sizes ranging from 400μm^2 to 1600 μm^2. The electrodes are carried on a boron diffused silicon substrate, 70 μm wide and 15 μm thick. Polysilicon conducting lines, carried by a flexible silicon cable, connect the sites to gold bond pads. Microwires are ultrasonically bonded to the bond pads and to a microtech connector. Epo-tek epoxy electrically insulates the wires and mechanically protects the bonds.

B. Surgical Procedure

The animals were handled in compliance with guidelines set by the University of Michigan Committee on Use and Care of Animals, State and Federal regulations, and the standards of the Guide for the Care and Use of Laboratory Animals. The electrode sites were activated to 30 mC/cm^2 by applying slow (1 Hz) voltage square wave to the electrode [1]. The probe was sterilized with ethanol. The guinea pig was anesthetized with a 1 : 1 mixture of ketamine : xylazine. Dental acyrlic was used to stabilize three 316 stainless steel (SS) screws implanted into the skull. Two screws were used for electrochemical testing and the third screw was used as a return electrode for current pulsing. 316 SS is resistant to corrosion, unlike other grades of stainless steel. Its use as a reference electrode is validated by the stable peak potentials in cyclic voltammagrams, indicating a fairly stable reference voltage throughout the implant period. The screw that served as counter electrode had a surface area exceeding 10^7 μm^2. The impedance of this electrode *in vivo* was less than 1 kΩ at all frequencies so the additional impedance added by the counter electrode was considered negligible. A craniotomy was performed with a dremel drill to expose the cortex. A small portion of dura was removed (the silicon probes cannot penetrate dura mater). The percutaneous connector was affixed to the skull with dental acrylic. The probe was then manually inserted into the neural tissue. A chamber was built around the implant and the chamber was filled with sterile agar to a level that covered the cable. After the agar solidified, dental acrylic was used to seal the implant.

C. Experimental Protocol

Stimulation began after a 10 to 17-day recovery period. Up to four electrodes were selected for testing, with one electrode reserved for an electrical control site (electrochemical tests but no pulsing) and one site reserved for a histological control (no electrical testing whatsoever). Biphasic current pulses (variable magnitude, 100 μs/phase, 250 pulses/s) were applied monopolarly for two hours on five consecutive days. Between pulses the electrode either floated or was set to a potential of 300 mV versus the 316 SS electrode. The *in vivo* resting potential of the iridium oxide was typically between 150 and 200 mV versus 316 SS, so the 300 mV positive bias placed the oxide in a more conductive state [4]. When the electrodes floated, anodic first pulses were used. When the positive bias was applied, cathodic first pulses were used. EIS and CV data were collected

on each stimulated site and one unstimulated, electrical control site before and after the two hours of stimulation. Cyclic voltammagrams were collected at scan rates of 100, 250, 500, and 1000 mV/s [20]. The voltage limits were −600 to +900 mV versus the 316 SS electrode (these limit were set inside the water window, i.e., the potentials at which hydrolysis would occur). EIS data was measured from 1 Hz to 1 MHz using a 15-mV rms sine wave (a voltage verified to be in the linear range of the electrode). The dc potential was set to 300 mV versus 316SS. The measurement system included a potentiostat (EG&E 283), a frequency response analyzer (EG&G 1025), and a 486 PC. The PC controlled the experiments via GPIB, with EIS software (EG&G 398) and CV software of our own design (LabVIEW, National Instruments). The activated iridium stimulation site (working) and two 316 SS screws (counter and reference) formed a three-electrode "test-cell" for electrochemical measurement. A constant current source of our own design was used to pulse the sites. The current source had blocking capacitors to ensure charge balance. The current source measured both the output current and the back voltage. The current source was interfaced with the PC via an analog input/output board (AT-MIO16F-5, National Instruments) under software control. A LabVIEW program was written to control the current pulsing and record the back voltage intermittently throughout the stimulation period.

D. Histology

Animals were sacrificed 4–5 weeks after the last day of stimulation. Analysis was performed on tissue and the explanted electrode. After sacrifice, the animal was fixed with 4% paraformeldehyde, the probe was explanted, the tissue of interest was dissected and embedded in JB4 glyco methacrylate plastic (Polysciences, Inc., Warrington, PA). Tissue slices were cut from the block using a Leitz microtome at a thickness of 2–3 μm. The sections were stained with paragon, which selectively stains nuclei. When possible, the probe was explanted after sacrifice and tissue fixation, and then analyzed with an electron microscope (ISI 130 or Electroscan ESEM). The ESEM was instrumented with a system that allowed an elemental analysis of the sample under test.

III. Results

A total of 25 electrode sites in seven animals were tested in the manner described (i.e., chronic pulsing with electrochemical testing). Electrochemical tests indicate consistent changes in the impedance spectrum as a result of current pulsing. The impedance in the 100 Hz to 100 kHz range generally decreased as a result of stimulation, while the low-frequency impedance (<100 Hz) increased. The latter change can be correlated with CV data. In spite of these changes, the back voltage was generally stable (i.e., the magnitude of the voltage did not change) throughout a stimulation period. EIS data from first two weeks of implantation suggests that encapsulation of the device caused an increase in impedance during the post-operative recovery period. Modeling the interface with circuit parameters allowed us to gain further insight into the physical changes at the interface reflected in the impedance spectrum. The 100 Hz–100 kHz range of the model corresponds to the Faradaic reactions within the iridium oxide. The low-frequency impedance was dominated by the impedance of the iridium oxide film. Experimental data was used to estimate model parameters for these two regions.

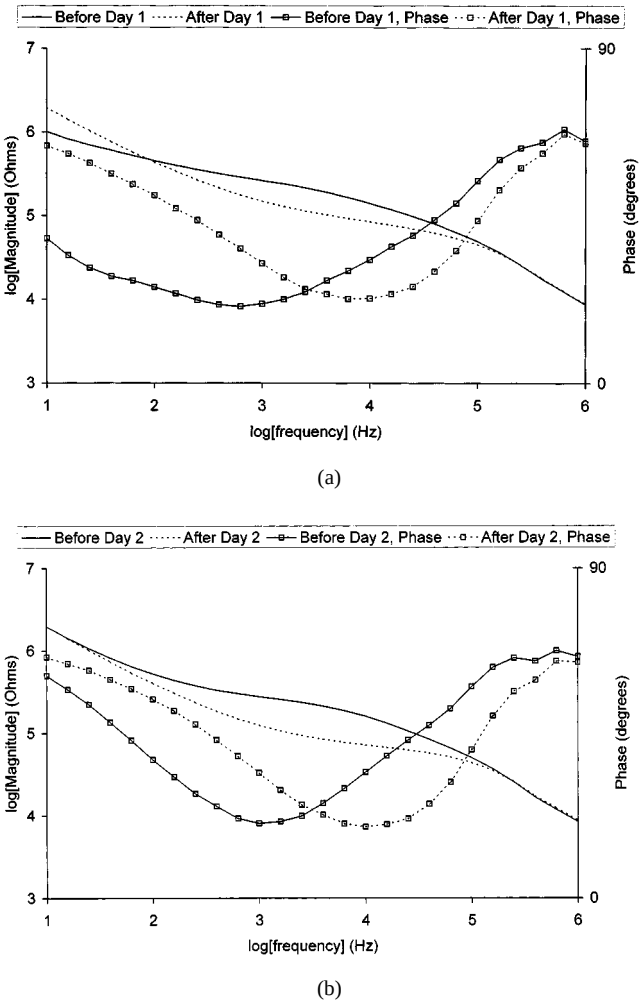

Fig. 1. Impedance magnitude and phase spectra before and after pulsing on (a) Day 1 and (b) Day 2.

A. Chronic Stimulation Experiments

The general appearance of the impedance data matched what other investigators have seen *in vitro* ([11], [21]). Typical results for two days of stimulation are plotted (Fig. 1). The general trends for the impedance spectra before and after stimulation are summarized below for three frequency regions.

1) Low-frequency impedance magnitude (below 100 Hz) increases after the first day of stimulation and remains at the increased level. Impedance phase in this region indicates a more capacitive impedance (i.e., the phase is closer to 90).
2) Mid-range-frequency impedance magnitude (100 Hz–100 kHz) decreases temporarily after stimulation but returns to prestimulation levels by the next day of testing. Changes in phase follow this same trend.
3) High-frequency impedance magnitude and phase (over 100 kHz) changes little.

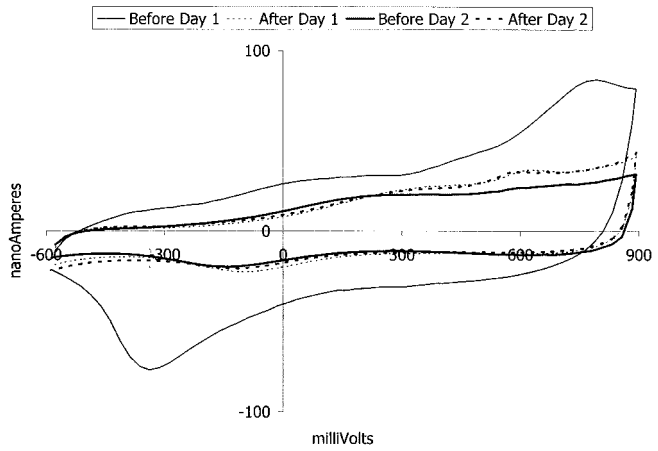

Fig. 2. Cyclic voltammagrams of two days of chronic *in vivo* testing.

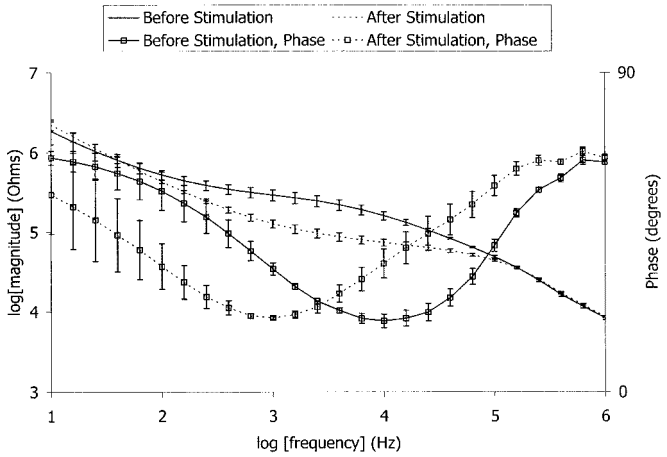

Fig. 3. Averaged impedance magnitude and phase spectra from one week of stimulation. Error bars equal to one standard deviation.

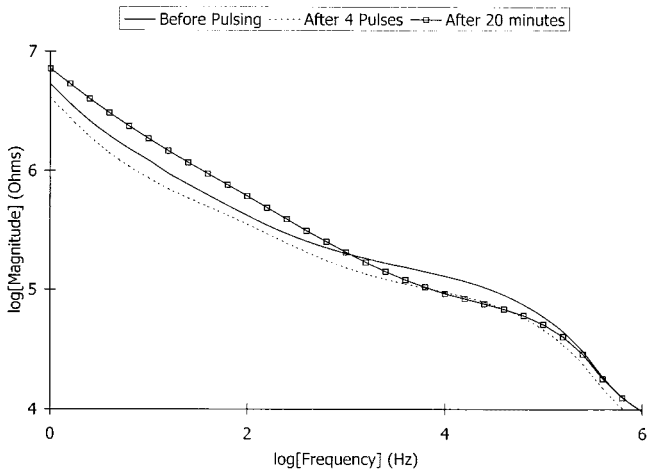

Fig. 4. Impedance magnitude spectra—before pulsing, after four pulses, and after two minutes of pulsing.

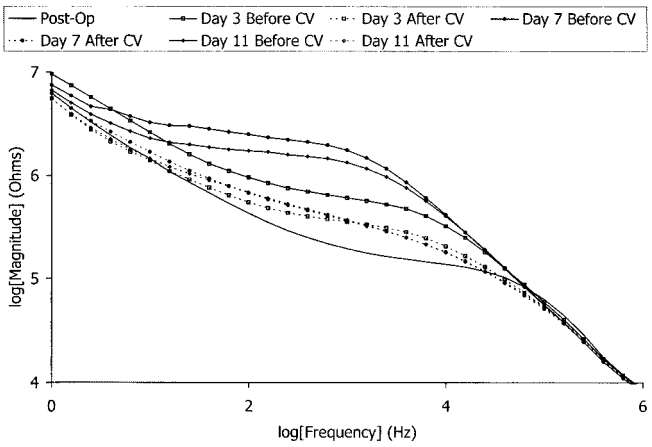

Fig. 5. Impedance magnitude spectra during two-week post-operative period.

CV data that correspond to the EIS data (Fig. 1) are shown in Fig. 2. The shape of the CV is altered and the value of Q_{cap} decreased after the first day of pulsing, after which the CV data change little. The change in the CV, therefore, appears to correlate with the low-frequency impedance change. This makes sense, because the ramp wave used for CV testing is a slow wave (i.e., its frequency content is concentrated in the low-frequency range). Finally, the electrical control sites (sites that were not pulsed) showed no change in either impedance or charge storage that correlated with electrical stimulation, ruling out any systematic changes caused by current pulsing.

The EIS data taken both before and after stimulation sometimes showed remarkable consistency throughout a whole week of testing (Fig. 3). For 90% of the experiments, the mid range impedance magnitude values (after stimulation) for the five days of testing varied less than 10%. Additionally, the qualitative observation of an impedance magnitude decrease in the 100 Hz–100 kHz range after stimulation was noted for every electrode tested.

Neither the impedance magnitude increase at low frequencies nor the impedance magnitude reduction at mid-range frequencies appeared to have a significant impact on the back voltage. Initially, the back voltage appeared to be relatively unaffected by the impedance changes. However, measuring the back voltage requires the application of high amplitude current pulses. This results in the interface properties changing after only a few pulses. Since the recorded back voltage was the average of 50 pulses, the change in the first few pulses was not initially visible. However, an analysis of the effects of just a few pulses demonstrated how the electrical properties are affected (Fig. 4).

It has been shown that the encapsulating tissue sheath that surrounds an implant will affect the electrical characteristics of the electrode-tissue system [22]. In these experiments, we allowed a two-week surgical recovery period, during which time the impedance increased dramatically. Some experiments were run to determine the time course of the impedance magnitude increase. The same implant and measurement protocols were followed as described above except only EIS and CV tests were run. Also, EIS tests were run before and after CV testing, since it was noted that CV testing could affect the impedance. A six-site probe was implanted as described previously. By day 3, impedance magnitude had increased significantly over post-op values (Fig. 5). The impedance magnitude before CV testing was high and somewhat inconsistent. CV testing lowered the impedance magnitude to a consistent level, suggesting that

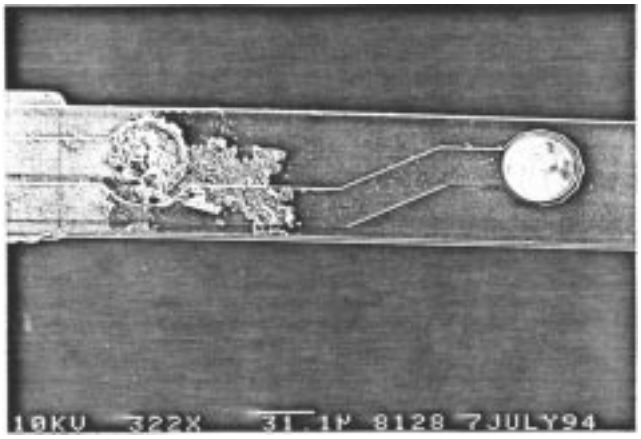

Fig. 6. SEM of explanted probe. The site on the left was used for chronic stimulation. The site on the right not stimulated. Analysis of similar films on other probes showed that the film was organic.

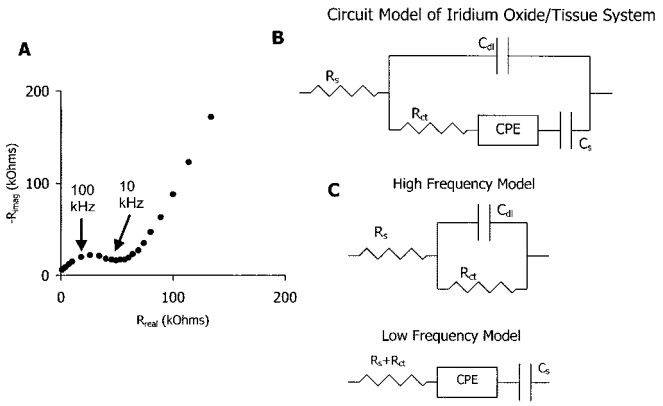

Fig. 7. (a)A circuit model can be used to predict the behavior of iridium oxide. (b) The impedance locus of iridium oxide has two distinct sections. (c) The circuit model of the electrode-tissue system can be broken down into two parts, one part that explains the semi-circle seen at high frequency, and a second part that explains the trajectory seen at low frequency.

cycling the electrode potential altered the interface in some way. The electrode appeared to be unaffected by encapsulation since the CV's were relatively stable throughout the two-week recovery period.

B. Histology

Histology was available from these experiments and a number of earlier chronic stimulation experiments that did not include the extensive electrochemical testing. Eight probes (containing 34 individual electrodes) were explanted in a sufficiently sound structural condition that allowed analysis of the probe. It was noted that an organic film selectively adhered to sites that had been used for stimulation (Fig. 6). A similar film was noted on 15 of the 22 sites pulsed with current and on two sites used only for CV testing. The film was determined to be organic by performing elemental analysis on the area. This analysis showed a significantly higher level of carbon and oxygen in the film compared to electrodes that had not been pulsed. Ten sites that were limited to EIS testing or no testing showed no adherent film. The tissue slices revealed no pattern of damage correlated to stimulation. Cells appeared normally shaped and no obvious decline in cell population was noted, though this was not studied quantitatively.

C. Circuit Models of the Electrode-Tissue System

1) Model Definition: Others have proposed a circuit model of iridium oxide [23]. A similar model to fit the data in these experiments is shown schematically [Fig. 7(b)]. R_s is the resistance of electrolyte and cabling. C_{dl} is the capacitive double layer between the iridium metal and ions in solution. The charge transfer reaction in the iridium oxide (1) is represented by R_{ct}. These first three components shape the high-frequency impedance. Since high-frequency impedance is considered independent of frequency, circuit parameters do fairly well modeling these current flow processes. The low-frequency impedance is highly frequency dependent, making it more difficult to model with discrete circuit components. Instead distributed networks that can be expressed in closed mathematical form are used to model this impedance. An example of this is the Warburg impedance [24]. A constant phase element (CPE) is a generalized Warburg that is present in the impedance of iridium oxide. Finally, C_s represents the charging of the entire oxide film. Unlike the model of Aurien-Blajeni *et al.*, no parallel resistance was evident in this data, even at frequencies as low as 1 mHz.

2) Model Parameter Estimation: Circuit model parameters were estimated from the experimental data. The initial estimates were made graphically from the intercepts, peaks, and slopes on the impedance locus plot. Then an iterative curve fitting routine was used to refine the estimates. The impedance locus in Fig. 7(a) exhibits a semicircle associated with the high-frequency portion of the model (R_s, R_{ct}, C_{dl}) as well as a straight line trajectory which is attributable to CPE and C_s, which dominate the impedance at low frequency. The component values for the entire system were determined by modeling these two portions (high frequency and low frequency) separately, effectively breaking the model of Fig. 7(b) into two parts, as shown in Fig. 7(c). This approach assumes that at high frequency, C_s and CPE are effectively short circuits, leaving the R_s in series with $R_{ct}||C_{dl}$. Furthermore, it is assumed that C_{dl} is an open circuit at low frequencies and the circuit reduces to the series combination of components shown. These assumptions appear to be valid, since the two geometric shapes in the locus (the semicircle and the straight line) are distinct.

R_{ct} is the parameter associated with the flat region of the impedance magnitude spectrum between 100 Hz and 100 kHz. Therefore, it is also the model component related to the transient change in impedance noted earlier. R_{ct} changed consistently as result of current pulsing. For example, during one week of testing of an 800 μm^2 electrode, R_{ct} averaged 210 kΩ before stimulation and 73 kΩ after stimulation. A decrease in R_{ct} suggests that pulsing results in a more efficient charge transfer process.

The model parameter CPE tracked the low-frequency impedance, although these results were not as consistent as those for R_{ct}. The CPE will first be discussed generally, and then the model results will be considered. The CPE is a mathematical quantity that represents an infinite network of resistors and capacitors [25]–[27]. A good example of a distributed network is a transmission line. The impedance of a uniform transmission line

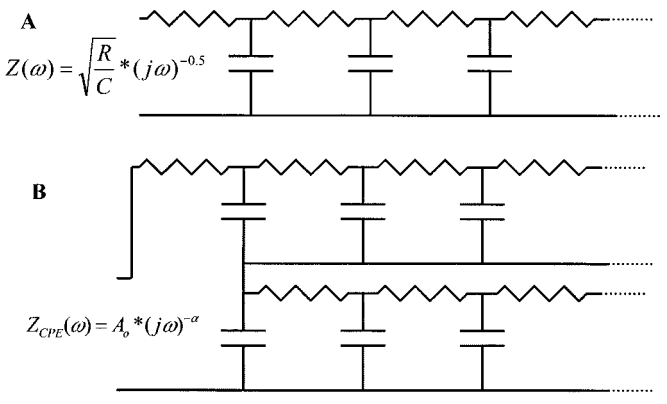

Fig. 8. Distributed networks showing the effect of branching on mathematical representation of pore impedance.

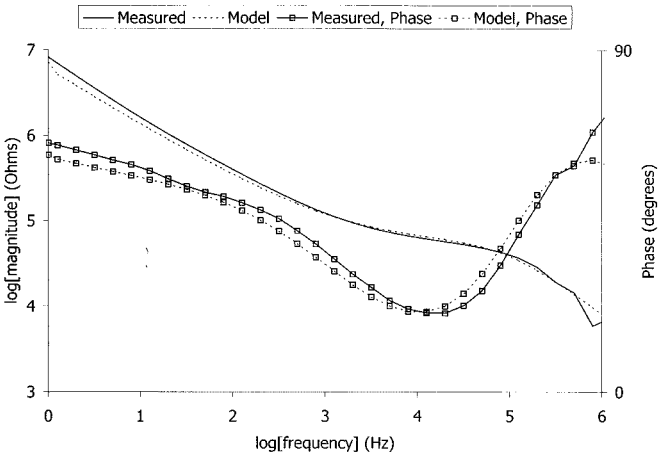

Fig. 9. Measured impedance magnitude and phase versus modeled impedance magnitude and phase.

(uniform because the longitudinal resistance and shunt capacitance are constant) is shown mathematically and schematically in Fig. 8(a). The frequency-dependent impedance of electrodes (i.e., the Warburg impedance) has this form with $\alpha = 0.5$ corresponding to a constant phase of 45° [24].

The rough, porous surface of iridium oxide adds complexity and nonuniformity to the frequency-dependent impedance. The CPE for the iridium oxide circuit model represents the impedance that ions encounter when flowing through the porous iridium oxide structure. If it is assumed that all the pores are uniform cylinders, then the impedance of the pores will be have the same form as the transmission line impedance. However, the pores are not perfectly cylindrical, but form a more tortuous path, with channels converging and diverging [12]. Therefore, the longitudinal resistance and shunt capacitance will vary throughout the conduction path resulting in a phase that is constant, but not necessarily 45°. It has been shown how pore branching can affect the phase of the CPE [27]. The effect of pore branching is shown in Fig. 8(b). A_o affects the magnitude of the impedance while α affects both the magnitude and nature of the impedance [i.e., capacitive (α closer to 1) versus resistive (α closer to 0)]. Typically, the models of *in vivo* data have shown $\alpha = 0.7$, with a range from 0.4–0.9.

A correlation can be made between CPE parameter values and charge storage. CPE impedance is most visible at low frequencies and it was shown earlier that charge storage is related to low-frequency impedance. Both A_o and α increase as charge storage decreases. A dramatic change in charge storage capacity was noted earlier. A typical case when Q_{cap} decreased from 0.32 μC to 0.1 μC, A_o increased from 2.8×10^6 to 5×10^7 and α increased from 0.43 to 0.74. Earlier data suggests that current pulsing results in a lower Q_{cap}, meaning the capacity to flow current through Faradaic reactions is diminished. This would agree with the system becoming more capacitive, as indicated by an increase in α.

3) Model for System Impedance: The model parameters for a particular EIS data set were assembled to form an equation for impedance (2). This equation was used to estimate the impedance spectrum. The comparison between measured impedance and predicted impedance is

$$Z(\omega) = R_s + \frac{1/(j\omega C_{dl}) * (R_{ct} + A_o(j\omega)^{-\alpha} + 1/(j\omega C_s))}{1/(j\omega C_{dl}) + R_{ct} + A_o(j\omega)^{-\alpha} + 1/(j\omega C_s)} \quad (2)$$

shown in Fig. 9. Since the model parameters used to predict the spectrum were based on the measured data, this result is not surprising. However, the close match supports to the validity of the model and the goodness of fit for the parameter values.

The impedance equation (2) can be used to predict back voltage for an arbitrary current pulse shape. Previous attempts at back voltage prediction used *in vitro* models, and did not compare model results with measured data [23]. The back voltage predictions were generated by transforming the impedance spectrum to the time domain to form an impulse response and then convolving the result with a current pulse input using a MATLAB routine (Mathworks, Natick, MA). Model parameters for the impedance equation were derived from EIS data measured after pulsing. Prior to EIS measurements, back voltage was measured for two biphasic pulses of different magnitude and duration (Fig. 10). The plots show that the simulated back voltage matches the measured back voltage at the shorter pulse duration, but exceeds the measured back voltage, particularly toward the end of the positive phase, at the longer pulse duration. This is most likely due to the nonlinear nature of the electrode impedance at low-frequency. Fig. 11 demonstrates how the impedance magnitude spectra is dependent on the excitation signal at low frequency. This behavior helps explain why the model, generated with small signal data, will lose accuracy simulating a large signal that contains more low-frequency components.

IV. Discussion

It was shown that electrical stimulation modified the characteristics of the metal-tissue interface in a consistent fashion. High intensity current pulsing did alter the electrode. Impedance magnitude at mid-range frequency (100 Hz–100 kHz) is lowered temporarily as a result of pulsing. Typically, by the next day, impedance in this range will have again increased. It is theorized that current pulsing improves the efficiency of the oxidation/reduction reactions in the iridium oxide. This effect is considered an *in vivo* phenomenon. This conclusion is supported by in vitro tests that show no change in impedance in this range when an electrode is pulsed in phosphate buffered saline.

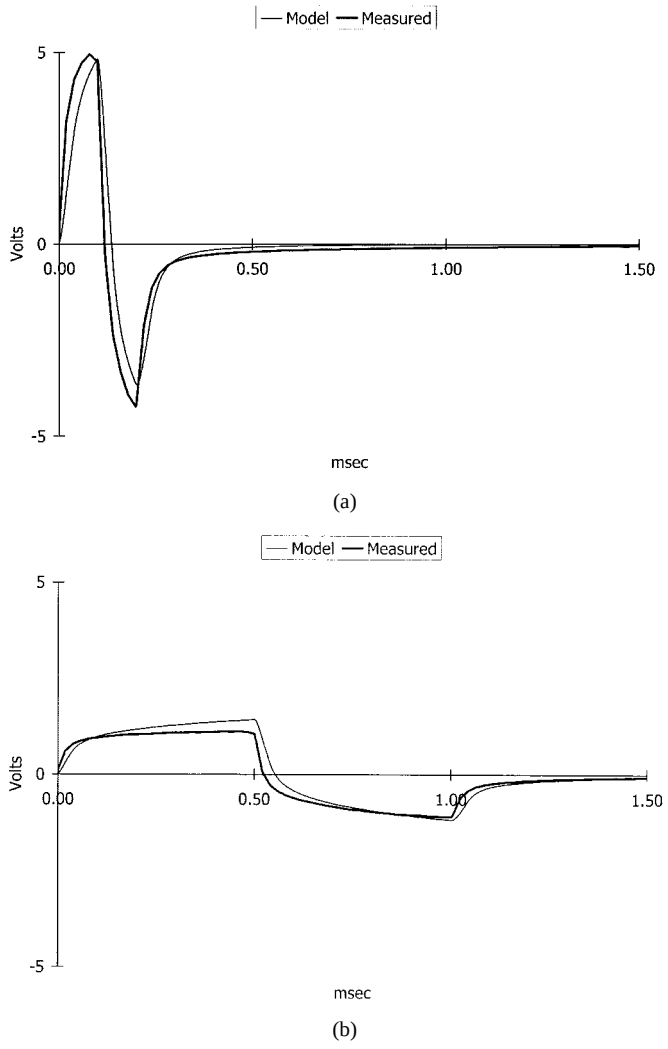

Fig. 10. Measured and modeled back voltage for 5 nC of charge delivered with a short (a) and long (b) pulse. Back voltage decreases with increasing pulse width. The model fairs poorly toward the end of long pulses, but otherwise predicts the back voltage fairly well.

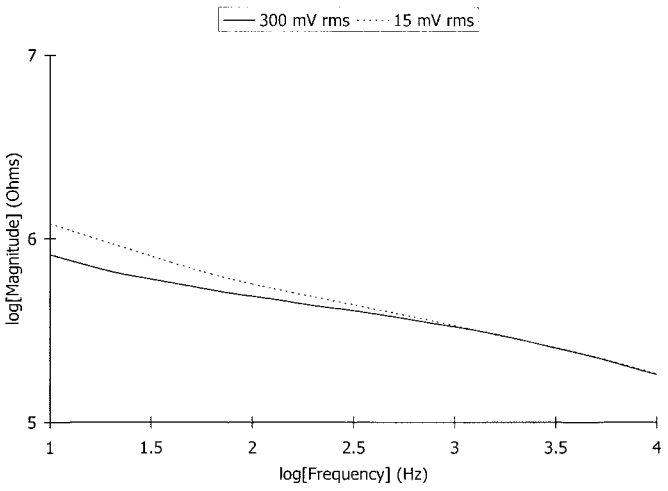

Fig. 11. Impedance magnitude spectra showing nonlinear nature of electrode impedance.

Current pulsing changes the low-frequency (<100 Hz) impedance also. This impedance range increased permanently, after one or two days of stimulation. A reduction in charge storage capacity correlated with this change, which implies a reduction in the maximum current magnitude safely injectable. The diminished charge storage capacity is troubling and difficult to explain. The pulses applied to the electrodes were not of such great magnitudes that the oxide should be damaged. In fact, current pulses were kept within the recommended limits, unless the point of the test was to cause damage. However, Q_{cap} invariably declined with pulsing, although rarely to the point where the injectable charge limits were exceeded and with no concurrent increase in back voltage. In fact, a significant amount of charge could still be safely injected even though Q_{cap} had diminished. Biphasic current pulses of 50 μA, 100 μs/phase were used on the electrode whose data was shown earlier (Figs. 1 and 2), resulting in a total of 5 nC delivered to the electrode during every pulse phase. A safe (within the water window) measure for injectable charge with a current pulse has been estimated to be approximately 10% of charge storage capacity [4]. In this case the lowest value for Q_{cap} is 63 nC, which allows 6.3 nC to be safely injected. Therefore, 5 nC appears to be a safe charge/phase. Additionally, this amount of charge is large enough to elicit a neural response from a penetrating, cortical electrode [28].

The experiments when charge storage was preserved for some part of the week of stimulation correlate to large sites (1200 μm^2 and over) and the use of a positive potential bias between pulses. Placing iridium oxide sites at a positive potential (about 300 mV versus 316SS) has been shown to increase the maximum safe charge limit [4]. Therefore it is recommended that these considerations be included in the design of active devices. It is also recommended that active recording devices include some means of outputting current in order to reduce the impedance if necessary.

Others have reported tissue accumulation on pulsed electrodes [29], [30]. The presence of a film at first seems to suggest increased impedance for pulsed electrodes (whereas the electrical data indicates the opposite). However, all this data really shows is that the electrode tissue interface was altered by chronic current pulsing. Since the current levels were within published guidelines for safe stimulation [9], the absence of any widespread tissue damage is not surprising.

Circuit models of the interface were used to analyze the experimental data and to predict the electrode potential in response to a current pulse. Individual elements of the circuit model changed in conjunction with changes in the impedance spectrum, indicating varying degrees of charge-carrying ability for those processes represented by the circuit elements. In a supported situation (i.e., the contents of the electrolyte are controlled), differences in impedance spectra were used to delineate different parts of the model [23]. Conversely, when consistent changes in model parameters are seen, it can be assumed that the electrode environment or the electrode itself is changing. The circuit model was used as a linear system function to produce electrode potential as output based on current pulse as input. It is known that the electrode-tissue interface is nonlinear, and no circuit model can be considered valid under all conditions of voltage and frequency. However, as suggested in a recent review by Geddes [18], over a limited range, circuit models can be applied to predict electrode performance. The

results in this paper suggest that at high frequencies, signals will give a linear response over a larger input signal range.

V. Conclusion

EIS and CV have been used to investigate the interface between iridium oxide and neural tissue. Chronic *in vivo* experiments were performed to assess the effects of stimulation on both electrode and tissue. Measurements of the impedance, charge storage, and back voltage have shown that the electrochemical properties of the interface are modified in a consistent way by electrical stimulation. Impedance data was used to generate circuit models of the electrode-tissue system. The model components were quantified and used to explain some of the experimental observations.

Acknowledgment

The authors would like to acknowledge the assistance of their colleagues at the University of Michigan, particularly J. Hetke, J. Wiler, B. Casey, and Dr. K. Wise. They would also like to thank Dr. T. Hambrecht and Dr. B. Heetdeerks of the Neural Prosthesis Program and Dr. R. Dubois of the National Center for Research Resources for their support and encouragement.

References

[1] L. S Robblee, J. L. Lefko, and S. B. Brummer, "Activated Ir: An electrode suitable for reversible charge injection in saline solution," *J. Electrochem. Soc.*, pp. 731–733, Mar. 1983.

[2] P. G. Pickup, "A model for anodic hydrous oxide growth at iridium," *J. Electroanal. Chem.*, vol. 220, pp. 83–100, 1987.

[3] M. Huppauff, "Valency and structure of iridium in anodic iridium oxide films," *J. Electrochem. Soc.*, vol. 140, pp. 598–602, 1993.

[4] X. Beebe and T. L. Rose, "Charge injection limits of activated iridium oxide electrode with 0.2 ms pulses in bicarbonate buffered saline," *IEEE Trans. Biomed. Eng.*, vol. 35, pp. 494–496, June 1988.

[5] J. C. Lilly, "Injury and excitation by electric currents: The balanced pulse-pair waveform," in *Electrical Stimulation of the Brain*, D. E. Sheer, Ed. Austin, TX: Hogg Foundation for Mental Health, 1961.

[6] S. B. Brummer and M. J. Turner, "Electrical stimulation of the nervous system: The principle of safe charge injection with noble metal electrodes," *Bioelectrochem. Bioeneng.*, vol. 2, pp. 13–25, 1975.

[7] R. H. Pudenz, W. F. Agnew, and L. A. Bullara, "Effects of electrical stimulation of the brain: Light and EM microscope studies," *Brain Behav. Evol.*, vol. 14, pp. 103–125, 1977.

[8] S. B. Brummer, L. S. Robblee, and F. T. Hambrecht, "Criteria for selecting electrodes for electrical stimulation: Theoretical and practical considerations," *Ann. N.Y. Acad. Sci.*, vol. 405, pp. 159–171, 1983.

[9] D. B. McCreery, W. F. Agnew, T. G. H. Yuen, and L. Bullara, "Charge density and charge per phase as cofactors in neural injury induced by electrical stimulation," *IEEE Trans. Biomed. Eng.*, vol. 37, pp. 996–1001, Oct. 1990.

[10] B. E. Conway, "Transition from "Supercapacitor" to "Battery" behavior in electrochemical energy storage," *J. Electrochem. Soc.*, vol. 138, no. 6, pp. 1538–1548, June 1991.

[11] B. Aurien-Blajeni, X. Beebe, R. D. Rauh, and T. L. Rose, "Impedance of hydrated iridium oxide electrodes," *Electrochimica Acta*, vol. 34, pp. 795–802, 1989.

[12] L. S. Robblee, "Studies of the electrochemistry of stimulating electrodes,", Final Rep., NIH Contract N01-NS-8-2313, 1991.

[13] S. J. Tanghe and K. D. Wise, "A 16-Channel CMOS neural stimulating array," *IEEE J. Solid-State Circuits*, vol. 27, pp. 1819–1825, Dec. 1992.

[14] D. B. McCreery, W. F. Agnew, and J. McHardy, "Electrical characteristics of chronically implanted platinum–iridium electrodes," *IEEE Trans. Biomed. Eng.*, vol. BME-34, pp. 664–668, 1987.

[15] D. A. Robinson, "The electrical properties of metal microelectrodes," *Proc. IEEE*, vol. 56, pp. 1065–1071, June 1968.

[16] M. Kendig and J. Scully, "Basic aspects of electrochemical impedance application for the life prediction of organic coatings on metals," *Corrosion*, vol. 46, no. 1, pp. 22–29, January 1990.

[17] V. A. Howarth and M. C. Petty, "Impedance spectroscopy of biomembrane Langmuir–Blodgett films," *Thin Solid Films*, vol. 244, pp. 951–954, 1994.

[18] L. A. Geddes, "Historical evolution of circuit models for the electrode-electrolyte interface," *Ann. Biomed. Eng.*, vol. 25, pp. 1–14, 1997.

[19] D. J. Anderson, K. Najafi, S. J. Tanghe, D. A. Evans, K. L. Levy, J. F. Hetke, X. Xue, J. J. Zappia, and K. D. Wise, "Batch-fabricated thin-film electrodes for stimulation of the central auditory system," *IEEE Trans. Biomed. Eng.*, vol. 36, pp. 693–704, 1989.

[20] U. M. Twardoch, "Integrity of ultramicro-stimulation electrodes determined from electrochemical measurements," *J. Appl. Electrochem.*, vol. 24, pp. 835–857, 1994.

[21] S. H. Glarum and J. H. Marshall, "The A-C response of iridium oxide films," *J. Electrochem. Soc.*, vol. 127, no. 7, pp. 1467–1474, July 1980.

[22] W. M. Grill and J. T. Mortimer, "Electrical properties of implant encapsulation tissue," *Ann. of Biomed. Eng.*, vol. 22, pp. 23–33, 1994.

[23] B. Aurian-Blajeni, "The numerical inversion of the Laplace transform to impedance spectroscopy," *J. Appl. Electrochem.*, vol. 22, pp. 553–557, 1992.

[24] M. Sluyters-Rehbach and J. H. Sluyters, "Sine wave methods in the study of electrode processes," in *Electroanalytical Chemistry: A Series of Advances*, A. J. Bard, Ed. New York: Marcel Dekker, 1970.

[25] J. R. Macdonald, *Impedance Spectroscopy: Emphasizing Solid Materials and Systems*. New York: Wiley, 1987.

[26] ——, "Note on the parameterization of the constant-phase admittance element," *Solid-State Ionics*, vol. 13, pp. 147–149, 1984.

[27] W. Scheider, "Theory of the frequency dispersion of electrode polarization. Topology of networks with fractional power frequency dependence," *J. Phys. Chem.*, vol. 79, no. 2, pp. 127–136, 1975.

[28] D. B. McCreery, L. A. Bullara, and W. F. Agnew, "Neuronal activity evoked by chronically implanted intracortical microelectrodes," *Exp. Neurol.*, vol. 92, pp. 147–161, 1986.

[29] W. F. Agnew, "Histopathologic evaluation of prolonged intracortical electrical stimulation," *Exp. Neurol.*, vol. 92, pp. 162–185, 1986.

[30] X. Xue, "Acute and chronic behavior of stimulating electrodes," Ph.D. dissertation, Univ. Michigan, Ann Arbor, 1990.

James D. Weiland (M'97) received the B.S.E.E. degree from the University of Michigan, Ann Arbor, in 1988. After 4 years at Pratt & Whitney Aircraft Engines developing electronic control systems for jet engines, he returned to Michigan for graduate school, receiving the M.S. degree in bioengineering (1993), the M.S. degree in electrical engineering, systems (1995), and the Ph.D. degree in biomedical engineering (1997). His graduate work concerned neural stimulation and stimulating electrode materials. He completed a post-doctroral fellowship at the Wilmer Ophthalmological Institute at Johns Hopkins University, Baltimore, MD, from 1997 to 1999.

He is currently an Assistant Professor of Ophthalmology at Johns Hopkins University where his research involves the development of an implantable electronic retinal prosthesis for the completely blind.

Dr. Weiland is a member of the Engineering in Medicine and Biology Society, the Biomedical Engineering Society, Sigma Xi, and the Association for Research in Vision and Ophthalmology.

David J. Anderson (S'62–M'67) received the B.S.E.E degree from Rensselaer Polytechnic Institute, Troy, NY, and the M.S. and Ph.D. degrees from the University of Wisconsin, Madison.

After completing a postdoctoral traineeship with the Laboratory of Neurophysiology, University of Wisconsin Medical School, he joined the University of Michigan, Ann Arbor, where he is Professor of Electrical Engineering and Computer Science, Biomedical Engineering, and Otolaryngology.

Dr. Anderson is a fellow of the American Institute for Medical and Biological Engineering, a member of the Neuroscience Society, the Acoustical Society of America, the Association for Research in Otolaryngology, and the Barany Society.